InertialElectrostatic Confinement of Ionized Fusion Gases

Robert L. Hirsch

Citation: J. Appl. Phys. 38, 4522 (1967); doi: 10.1063/1.1709162
View online: http://dx.doi.org/10.1063/1.1709162
View Table of Contents: http://jap.aip.org/resource/1/JAPIAU/v38/i11
Published by the American Institute of Physics.

JOURNAL OF APPLIED PHYSICS VOLUME 38, NUMBER 11 OCTOBER 1967

Inertial-Electrostatic Confinement of Ionized Fusion Gases

ROBERT L. HIRSCH
ITT Farnsworth Research Corporation, Fort Wayne, Indiana
Received 13 March 1967; in final form 19 June 1967)

The nonmagnetic, inertial-electrostatic confinement of ionized gases in spherical geometry is discussed theoretically, and associated experiments are described. Assuming monoenergetic ion and electron distribution functions, the Poisson equation for bipolar currents is solved numerically. The results indicate spatially periodic solutions which respresent the alternate formation of virtual anodes and virtual cathodes. Particle pressures are found to vary approximately as the inverse square of the radius and extremely high electric fields are indicated. Near the center of the spherical cavity, there exists a high-density, high-energy region, which may be of controlled fusion interest.

The experimental apparatus consists of a hollow spherical cathode concentrically placed within a spherical anode on which six ion guns are located. Steady, reproducible operation up to -150 kV and 60 mA yields a copious neutron emission, a part of which originates from a luminous spherical region within the cathode. After crowbar of the main power supply, approximately 10^{16} particles are released from within the cathode. This number is significantly greater than the 10^{12}–10^{14} ions/cm^{-3} calculated from the fusion rate. The difference is attributed to the formation of two or more virtual anodes. A bremsstrahlung collimation study indicates a spatially periodic emission pattern, suggesting the formation of at least two virtual anodes, the outer of which is about 2.5 cm in diameter. No instabilities have been observed.

I. INTRODUCTION

Over thirty-five years ago Farnsworth[1] noted the existence of a localized glow at the center of a spherically symmetric, high-vacuum multipactor tube.[2] He later reasoned that radially focused electron currents were producing a space-charge potential well in the hollow anode cavity. This well was confining and concentrating ions which were produced from residual gas.

Although the operation of the multipactor tube has not been studied in detail, the concept of confinement in a dynamically produced potential well has received further consideration. In the mid-1950's Farnsworth suggested that this technique might be utilized to confine and concentrate ions into a small volume where an appreciable number of nuclear fusion reactions could occur. At that time ITT initiated a modest program to investigate this technique of fusion-gas confinement. The results of recent theoretical and experimental efforts are presented below.

II. BACKGROUND

The phenomena of space-charge and particle trapping in potential wells are well known. Child[3] investigated space-charge effects in a plane-parallel diode, after which Langmuir and his co-workers[4] studied other electrode configurations. Arbitrary initial conditions have been considered.[5,6] The extension to bipolar currents in plane geometry was made by Langmuir,[7] Muller-Lübeck,[8] and Howes.[9] Studies of cesium diodes[10] and electrostatic propulsion devices[11] have further expanded our understanding of these problems.

The classic work of Bernstein, Greene, and Kruskal[12] has shown that a variety of distribution functions are compatible with the formation of electrostatic potential wells containing trapped particles. Recently, Berk[13] and Drummond[14] have suggested that the unstable two-stream system relaxes to a quasistable potential well. Their work indicates possible stability in other two-stream configurations.

Tuck, Elmore, and Watson[15] analyzed a fusion device based upon particle confinement in spherical potential wells produced by circulating electrons. Their model assumed a spherically symmetric system in which electrons were radially directed towards the center at which a plasma was assumed to exist. Their analysis indicated that such a system would require prohibitively high power inputs to be of thermonuclear interest, and, furthermore, it would probably be unstable.[16] Subsequently, Tuck[17] expressed interest in a

[1] P. T. Farnsworth (private communication, 1964).
[2] A sustained, high-frequency, secondary-emission discharge.
[3] C. D. Child, Phys. Rev. **32**, 492 (1911).
[4] I. Langmuir, Phys. Rev. **2**, 450 (1913); Z. Physik **15**, 348 (1914); I. Langmuir and K. B. Blodgett, Phys. Rev. **22**, 347 (1923); **23**, 49 (1924).
[5] B. Salzberg and A. V. Haeff, RCA Rev. **2**, 336 (1938).
[6] C. E. Fay, A. L. Samuel, and W. Shockley, Bell System Tech. J. **17**, 49 (1938).
[7] I. Langmuir, Phys. Rev. **33**, 976 (1929).
[8] K. Muller-Lübeck, Z. Angew. Phys. **3**, 409 (1951).
[9] W. L. Howes, J. Appl. Phys. **36**, 2039 (1965).
[10] See, for instance, P. Burger, "The Opposite-Stream Plasma Diode," Stanford University Technical Report No. 0254-1, April 1964. P. Burger, D. Dunn, and A. Halsted, Phys. Fluids **8**, 2263 (1965).
[11] See, for instance, D. Dunn and I. Ho, *AIAA* J. **1**, 2770 (1963).
[12] I. B. Bernstein, J. M. Greene, and M. D. Kruskal, Phys. Rev. **108**, 546 (1957).
[13] H. L. Berk and K. V. Roberts, Sherwood Theoretical Meeting, 30–31 March 1967. Submitted for publication.
[14] J. E. Drummond, Sherwood Theoretical Meeting, 30–31 March 1967.
[15] W. C. Elmore, J. L. Tuck, and K. M. Watson, Phys. Fluids **2**, 239 (1959).
[16] Instability of the Ref. 15 model was also considered by H. P. Furth, Phys. Fluids **6**, 48 (1963).
[17] J. L. Tuck, *Proceedings of the Second United Nations International Conference on the Peaceful Uses of Atomic Energy* (United Nations, Geneva, 1958), Vol. 30, p. 6.

system wherein ions were substituted for electrons, but did not pursue the subject. Rasor[18] independently became interested in this method of trapping fusion gases and performed an analysis which was not published. Lavrentyev[19] considered the case of symmetric-ion and electron injection in plane and spherical geometry. Employing arbitrary distribution functions, he solved Poisson's equation. His solutions exhibited potential wells for various distribution functions of interest, i.e., parabolic, Gaussian, and Maxwellian. He did not, however, carry his analysis so far as to detail the shapes of the potentials.

III. THE CONCEPTUAL PICTURE

In order to facilitate an understanding of this particular approach, it is worthwhile constructing a conceptual model based on the essence of the theoretical results. Consider a spherical cathode concentrically surrounded by a spherical anode [Fig. 1(a)]. The cathode is assumed to be ion permeable, electron emissive on its interior surface only, and impermeable to electron flow into the interelectrode space. The anode is assumed to be uniformly ion emissive, and all ions are emitted with zero kinetic energy. Assume that all particle motions are radial, i.e., neglect scattering.

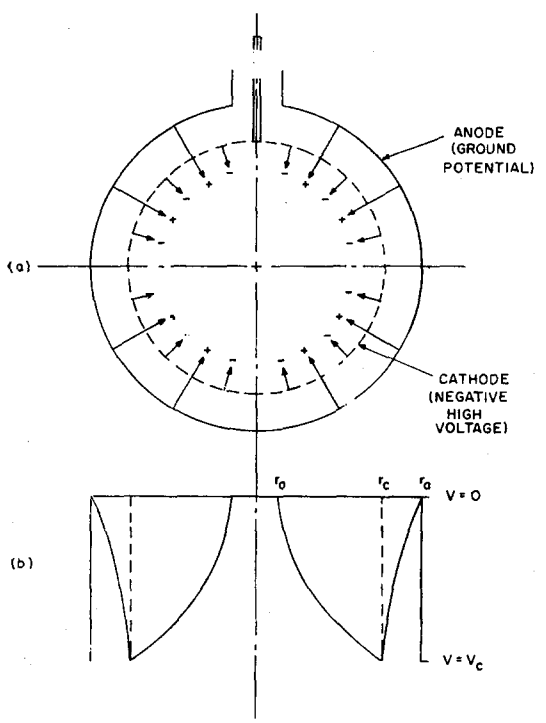

FIG. 1. The general arrangement and the potential distribution when ions only are present.

[18] N. S. Rasor (private communication 1960) and various internal memos, Atomics International, 1957).
[19] O. A. Lavrentyev, Ukr. Fiz. Zh. (U.S.S.R.) **8**, 440 (1963).

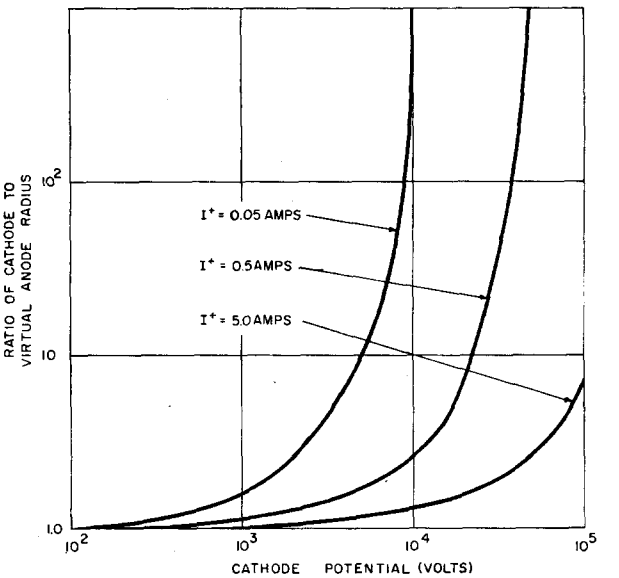

FIG. 2. Ratio of cathode to virtual anode radii as a function of D^+ ion current and cathode potential.

For the case of finite ion current and zero electron current, an ion space charge will develop within the cathode. At steady state this space charge will decelerate all incoming ions and cause them to reverse their motions at a finite radius r_0. These ions will then be accelerated outwards and will again be decelerated in the interelectrode space. In this manner a deep potential well is produced and maintained by circulating ions. The associated potential distribution can be calculated from a simple extension of the Langmuir–Blodgett[4] analysis of electron flow between spherical electrodes. This potential is shown in [Fig. 1(b)]. The potential at r_0 is that of the anode so that the shell at r_0 may be considered a virtual anode, i.e., it is a charge-saturated region from which ions are emitted in an outward direction.

For $D+$ ions at voltages and currents of thermonuclear interest, the cathode to virtual anode-radius ratios are shown in Fig. 2. Although the currents in the 10^4–10^5-V range appear high for a reasonable radius ratio, i.e., 10 to 10^3, it must be borne in mind that a highly open real cathode (90–95%) will permit many ion transits before loss to the cathode structure. For example, an external current of only 50 mA would be required for a circulatory current of 500 mA in a cathode permitting an average of ten ion transits (round trips). If this ion model could be realized experimentally, it would exhibit a negligible fusion rate, since the ion density is low where the ion energy is high, i.e., near the cathode.

If now electrons are permitted to flow from the cathode, they would be accelerated by the virtual anode towards the center of the tube. Once inside the virtual anode, they would be decelerated by their own

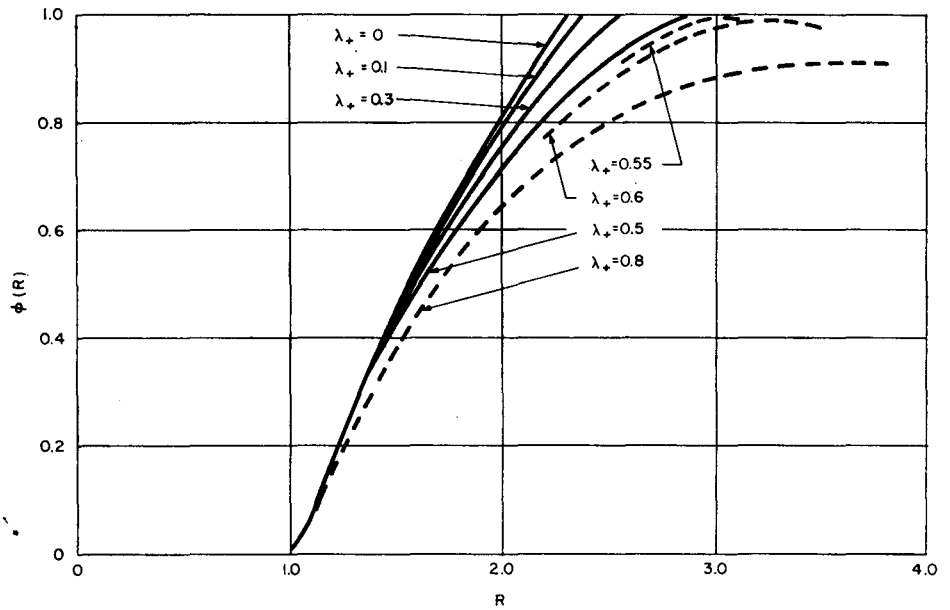

FIG. 3. Potential distributions at $K_+=1.0$.

space charge, and they would form a virtual cathode at $r_{vc}<r_0$. This negative space charge will cause ions from the virtual anode to be accelerated towards the center while also decreasing the radius of the virtual anode. In this manner a series of virtual electrodes can form, creating successively denser regions of high ion kinetic energies.

IV. THE ANALYSIS

For bipolar currents in spherical geometry, Poisson's equation is

$$(1/r^2)\,(d/dr^2)[r^2(dV/dr)]=4\pi(|\,\rho_e\,|-\rho_i). \quad (1)$$

Taking the zero of potential at the virtual anode, the conservations of energy become

$$\tfrac{1}{2}Mv_i^2=|\,eV(r)\,|, \quad (2)$$

$$\tfrac{1}{2}mv_e^2=e(V-V_0), \quad (3)$$

where V_0=the cathode potential. Conservation of charge becomes

$$I_{e,i}=4\pi r^2\rho_{e,i}v_{e,i}. \quad (4)$$

Next, normalize the radius and the potential,

$$\phi(r)=V(r)/V_0, \quad (5)$$

$$R=r/r_a, \quad (6)$$

where r_a=the radius of the virtual anode [note that $\phi(r_a)=0$]. Equation (1) then takes a form similar to that of Elmore, Tuck, and Watson,[15]

$$\frac{d^2\phi}{dR^2}+\frac{2}{R}\frac{d\phi}{dR}=\frac{K_+}{R^2}\{\phi^{-1/2}-\lambda_+(1-\phi)^{-1/2}\}, \quad (7)$$

where

$$K_+=\frac{I_i}{|\,V_0\,|^{3/2}}\left(\frac{M}{2e}\right)^{1/2}=\frac{4\pi r^2\rho_i\phi^{1/2}}{|\,V_0\,|}, \quad (8)$$

$$\lambda_+=(I_e/I_i)\,(m/M)^{1/2}. \quad (9)$$

For $\lambda_+=0$ Eq. (7) reduces to a form similar to that of Langmuir–Blodgett.[4]

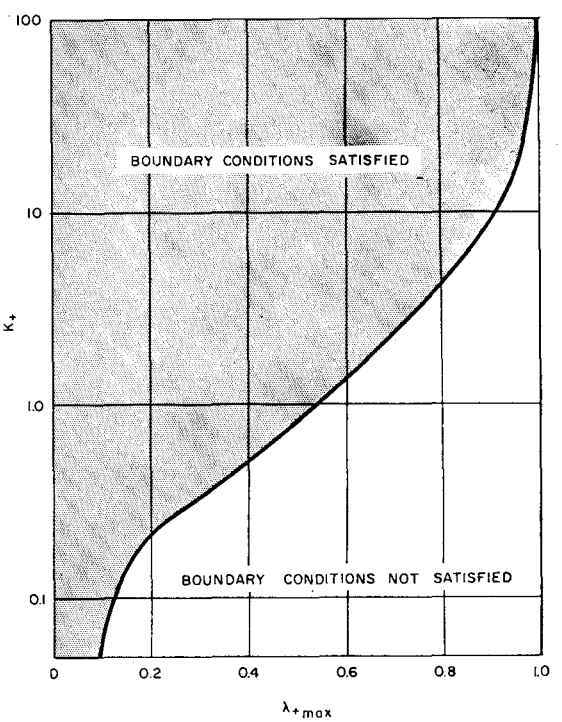

FIG. 4. Locus of λ_{+max} as a function of K_+, showing the region in which the boundary conditions are satisfied.

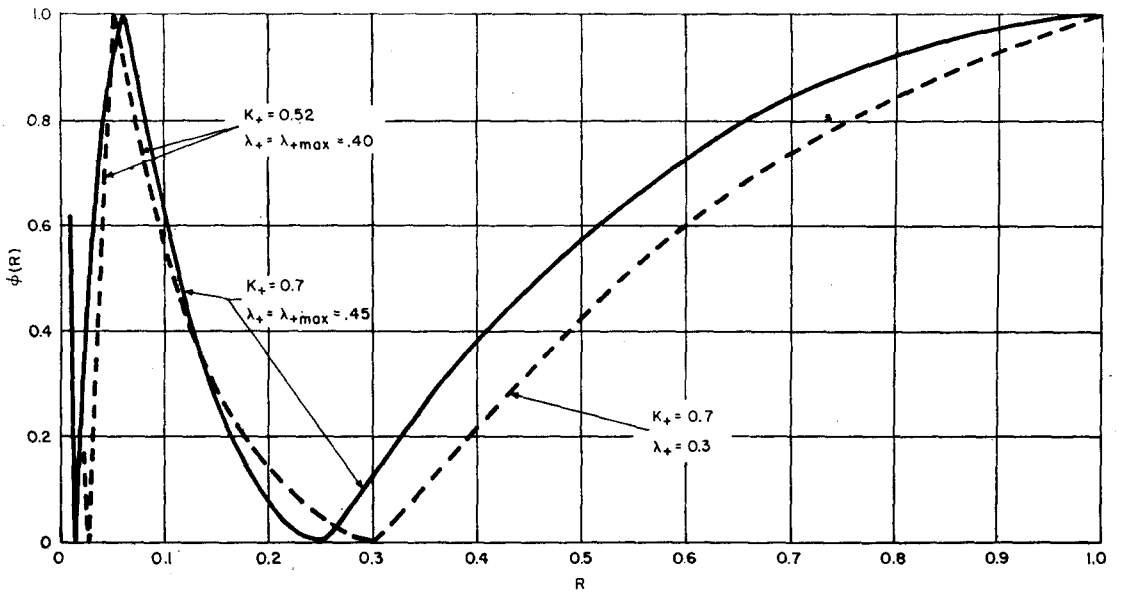

FIG. 5. Comparison of normalized potential distributions for $K_+=0.7$ at $\lambda_{+\max}$ and at 0.67 $\lambda_{+\max}$.

If the electrons had been considered as the primary particle the zero of potential would have occurred at the cathode and r_a would be replaced by r_c, the cathode radius. Equation (7) would be unchanged provided new constants were defined as follows,

$$K_e=(I_e/|V_0|^{3/2})(m/2e)^{1/2}, \tag{10}$$

$$\lambda_e=I_i/I_e(M/m)^{1/2}. \tag{11}$$

Note that

$$K_+=K_e\lambda_e, \tag{12}$$

$$K_e=K_+\lambda_+, \tag{13}$$

$$\lambda_+=(\lambda_e)^{-1}. \tag{14}$$

These relationships are of value in connecting adjacent regions.

Solutions of Eq. (7) between a virtual anode and an adjacent cathode (real or virtual) are of interest. These solutions lie in the regions $0\leq\phi\leq 1$ and $1\leq R\leq R_c$, where R_c is the cathode radius. Examination of Eq. (7) shows that the first term on the right-hand side will dominate the second term near $R=1$, i.e., $\phi\sim 0$. Neglect of the second term with respect to the first reduces the problem to the Langmuir–Blodgett[4] case. From their work an asymptotic solution of Eq. (7) can be obtained. In this notation this solution is

$$\phi\simeq(2.25K_+)^{2/3}(R-1)^{4/3} \qquad (R\sim 1). \tag{15}$$

In essence, this is merely a recognition of the fact that the ion space charge dominates the electron space charge near a virtual anode.

Equation (15) has been utilized to calculate initial conditions for numerical solutions of Eq. (7). Values of the initial radius, R_0, were chosen such that the resultant value of $\phi(R_0)$ gave a first term on the right-hand side of Eq. (7) which was greater than 100 times the maximum value of the second term. This condition was found to justify the use of the asymptotic solution. As a check on the initial values, an integration at $\lambda_+=0$ was made at each value of K_+, and the resultant values of R_c (the radius at which $\phi=1.0$) were compared with those calculated by Langmuir–Blodgett. The agreement was typically better than 1%.

Values for K_+ from 0.07 to 100 have been studied with $0\leq\lambda_+\geq\lambda_{+\max}$, where $\lambda_{+\max}$ is the maximum value of λ_+ for which the solution satisfies the boundary conditions. The integrations were performed on an Olivetti–Underwood Programma 101 desk-top computer.[20] The potential distribution at $K_+=1.0$ is characteristic of those at other values of K_+ and is shown in Fig. 3. In general, the following characteristics are evident:

1. The region in which ϕ and $d\phi/dR$ approach zero is relatively small.
2. The addition of electrons reduces the radius of the virtual anode in a fixed radius device.
3. A $\lambda_{+\max}$ exists at which the potential distribution becomes tangent to $\phi=1$. Values of $\lambda_+>\lambda_{+\max}$ result in distributions which do not reach $\phi=1$, i.e., they do not satisfy the boundary conditions but instead oscillate below $\phi=1$.

In plane-parallel geometry, Langmuir[7] noted that $\lambda\leq 1$ since the potential gradient at the anode surface

[20] Original program written by P. R. Adams, ITT Headquarters, New York, N.Y.

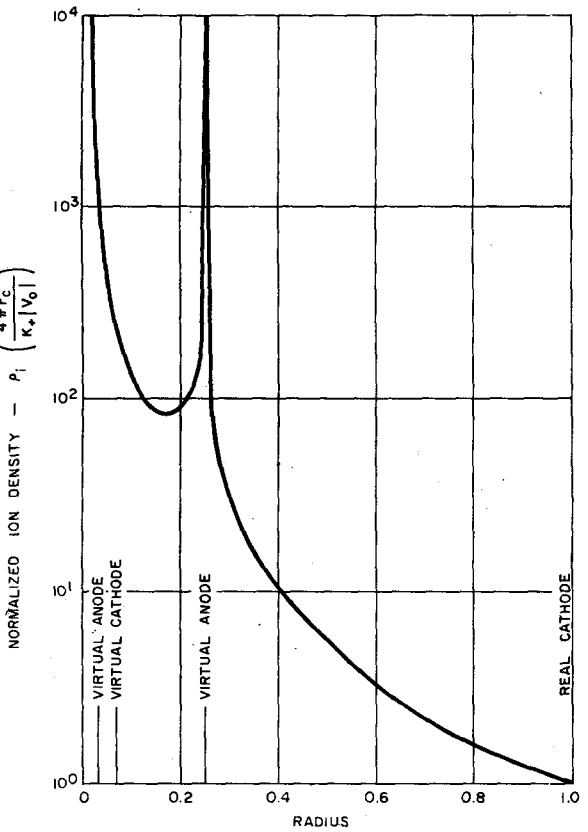

FIG. 6. Normalized ion density as a function of radius for $K_+=0.7$, $\lambda_+=\lambda_{+max}=0.45$

was proportional to $(1-\lambda)^{1/2}$. In spherical geometry radial focusing occurs and therefore λ_{+max} must be less than unity. The dependence of λ_{+max} on K_+ is shown in Fig. 4 where λ_{+max} is seen to decrease with decreasing K_+, i.e., increasing ratio of virtual anode to cathode radius.

In the region between the real cathode and the virtual anode any combination of K_+ and λ_+ to the left of the λ_{+max} curve will satisfy Eq. (7) and the boundary conditions. However, in the region between the first virtual anode and the inner virtual cathode, both currents are space-charged-limited, i.e., they satisfy a K_+, λ_{+max} condition. This condition coupled with the continuity of electron current between the regions is sufficient to determine the ion current in this adjacent region.

We are now in a position to establish the complete potential distributions. As an example, Fig. 5 shows two distributions at $K_+=0.7$. The first is at $\lambda_+=\lambda_{+max}=0.45$, and the second is at $\lambda_+=0.3=0.667\lambda_{+max}$. Both curves are spatially periodic with the period rapidly decreasing with decreasing radius. The tangencies to $\phi=0$ are points at which ions slow to zero velocity and are therefore referred to as virtual anodes. Similarly the tangencies to $\phi=1.0$ represent virtual cathodes. Farnsworth[21] has called this inertially separated, charged-particle structure a "poissor," since it represents an interesting solution of Poisson's equation.

Figure 6 shows the normalized ion density as a function radius which corresponds to the potential distribution shown in Fig. 5. As expected, the ion density goes to infinity at the virtual anodes. At the virtual cathode at $R=0.065$, the ion density is seen to be well over two orders of magnitude greater than it is at the real cathode.

In this ideal model with purely radial flow, a force balance exists at steady state since the inward and the outward currents of both particles are everywhere equal. In a plane electrostatic system it is well known that $E^2/8\pi$ balances the total particle pressure. In spherical geometry such a simple balance does not occur due to the effects of radial focusing.[22,23] In this simplified analysis the particle pressure is

$$P=n_e m v_e^2+n_i M v_i^2. \tag{16}$$

From eqs. (2), (3), (4), and (8),

$$P=[(K_+V_0^2)/2\pi r_c^2](1/R^2)\{\lambda_+(1-\phi)^{1/2}+\phi\}. \tag{17}$$

From the data of Fig. 5 at $K_+=0.7$ and $\lambda_{+max}=0.45$, the particle pressure was calculated from Eq. (17) and plotted in Fig. 7 along with $E^2/8\pi$ graphically determined from Fig. 5. Since the term in the brackets in Eq. (17) is of the order of unity, the particle pressure

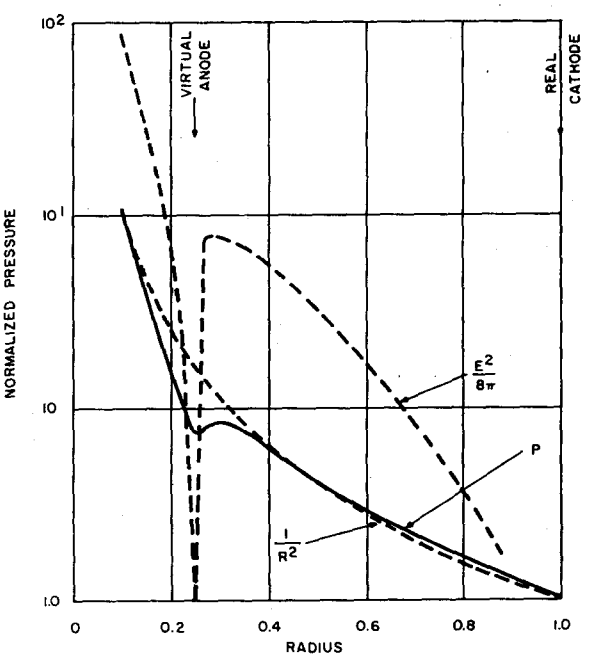

FIG. 7. Particle and electric field pressure vs radius for $K_+=0.7$, $\lambda_+=\lambda_{+max}=0.45$.

[21] P. T. Farnsworth, Patent No. 3,258,402, issued 28 June 1966, and patent applications pending.
[22] W. B. Thompson (private communication, 1967).
[23] A. Simon (private communication).

generally follows a $1/R^2$ dependence with the largest deviation occurring at the virtual anode. The electrostatic pressure increases drastically with decreasing radius but falls to zero at each virtual electrode. In this manner very high particle and electrostatic pressures are realized near the center of the sphere. It is this dense, high-pressure central region which is of interest to fusion physics.

It has been suggested that this concept may somehow be limited by the virial theorem. Recently, two independent analyses of the generalized electrostatic system[22,23] have been completed, and they have shown that no such limitation occurs.

V. FUSION-REACTOR CONSIDERATIONS

It is instructive to extract the important features of the model, make some reasonable assumptions, and thereby determine the general characteristics of an electrostatic fusion reactor. We assume for this analysis that the system is dynamically stable. Consider a small uniform, high-density region at the center of a poissor-like structure. The ion density in this region is n_0 while its radius is r_0. Taking the maximum cross section of the D–T reaction, the power output of this small region would be

$$P_0 \simeq 10^{-26} n_0^2 r_0^3 \quad \text{W}. \tag{18}$$

Assume that the center density is related to an ion current, I_0, at r_0 by

$$n_0 = I_0/4\pi r_0^2 v_0 e \tag{19}$$

Then the fusion power output becomes

$$P_0 \simeq 2\times 10^{-8} I_0^2/r_0 \quad \text{W}, \tag{20}$$

where I_0 is in amperes. Equation (20) emphasizes the fact that the "active" volume in an electrostatic machine would be a small, high-density region rather than a large, moderate density region, as in most magnetic devices. In a one-meter radius device, a central-region size of $r_0 = 0.1$ cm seems reasonable. At that size Eq. (20) indicates a total ion current of 2×10^5 A at $P_0 = 10$ kW.

But there is a direct conversion mechanism inherent to this concept. If of the order of a hundred kilovolts negative is applied to the cathode, a retarding field exists for the charged fusion products which enter the interelectrode space. Since any practical cathode must be of the order of 95% open, most of the charged fusion products will enter the interelectrode space and thereby deliver energy directly to the apparatus while the remainder will strike the cathode structure. This directly converted energy P_d is

$$P_d = \gamma P_0 (E_p/E_f) \cdot (E_g/E_p), \tag{21}$$

where γ is the cathode geometry factor (here taken as unity), E_p is the energy of the fusion charged particle, E_f is the total fusion-energy release, and $E_g = eV_g$ is the cathode potential energy. Substituting quantities appropriate to the D–T reaction and $V_g = 100$ keV,

$$P_d \simeq 5.7\times 10^{-3} P_0 \simeq 10^{-10} I_0^2/r_0. \tag{22}$$

The power input to the system is

$$P_{\text{in}} = I_g V_g = (I_{gc}/\nu)\, V_g, \tag{23}$$

where I_g is the ion current to the cathode (grid), I_{gc} is the ion current circulating through the cathode (not necessarily equal to I_0), and ν is the number of trips the average ion makes through the grid ($\nu = 10$ is considered reasonable).

Let us now differentiate between the ion currents at the center and at the real cathode and define the current amplification as

$$\eta = I_0/I_{gc}. \tag{24}$$

In the simplified model described above, η is unity since a constant ion current was assumed to exist across the whole anode [Eq. (4)]. The model, however, represents a first-order approximation in that it neglects energy spread and particle trapping in the potential wells. If the wells can be experimentally realized, binary collisions and collective interactions will deposit particles in them and these particles will remain trapped for very long times. Therefore, if trapping occurs, the particle pressures on opposite sides of virtual electrodes would not necessarily be equal. Although such a pressure discontinuity is intuitively disturbing, it is mathematically permissible, i.e., there are a variety of solutions to the Poisson and conservation equations which involve pressure discontinuities across virtual electrodes.[12] A well-known system in which this phenomenon occurs is the space-charge-limited diode.[5,6] On the cathode side of the virtual cathode both reflected and escaping electrons exist. On the anode side of the virtual cathode only the escaping electrons are present. Therefore, a particle-pressure discontinuity occurs at the virtual cathode.

We now consider a nonunity amplification factor and show that large values of η are necessary for a practical electrostatic fusion reactor. A power level of interest is that at which the input power is balanced by the directly converted energy, i.e., $P_d = P_{\text{in}}$. The current amplification then becomes

$$\eta \simeq 4\times 10^9\, P_0^{-1/2}. \tag{25}$$

Without particle trapping, i.e., all center current supplied from the real cathode, an excessively high power level would be required for the apparatus to power itself. On the other hand, an $\eta \simeq 4\times 10^5$ would provide self-sustaining operation at 100 MW.

This order of magnitude calculation is optimistic in that it neglects losses and is pessimistic in that it assumes the center region to be uniform rather than

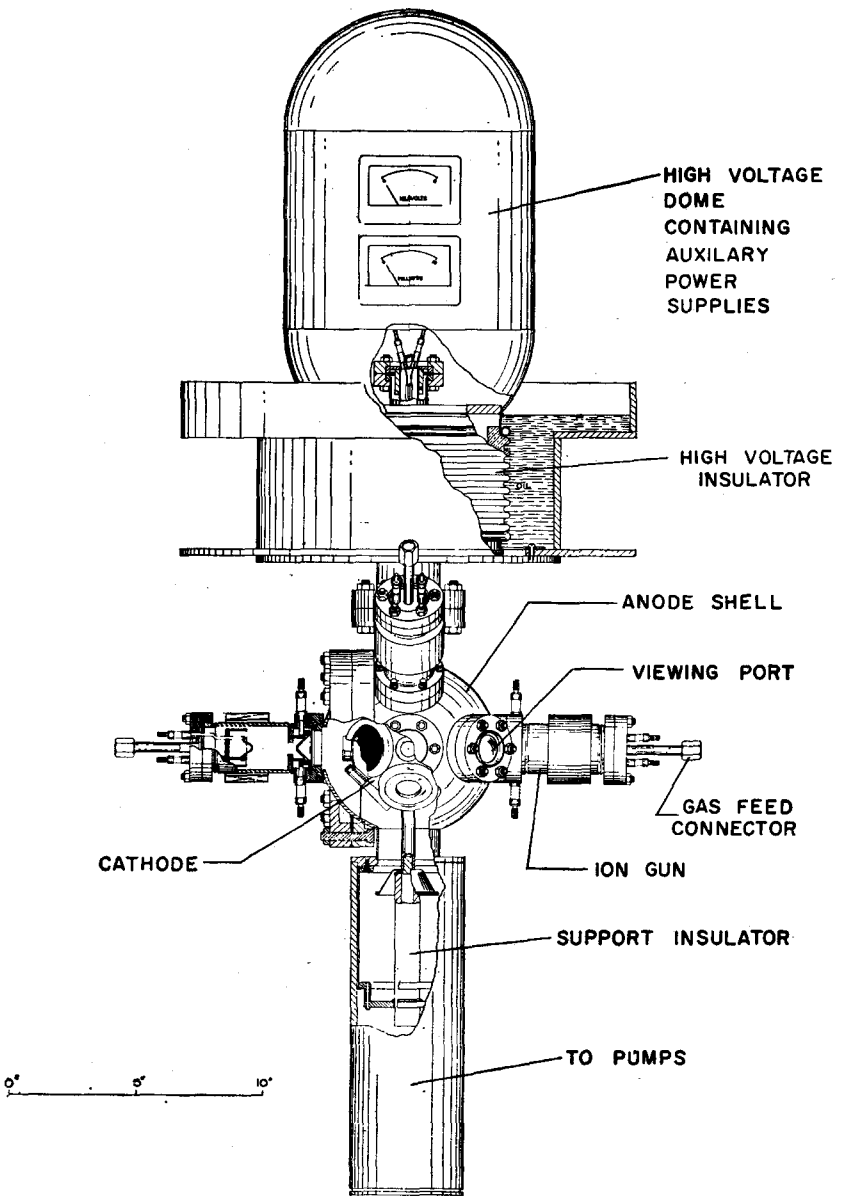

FIG. 8. The arrangement of a typical experimental device.

peaked at the center. It nevertheless draws attention to a necessary characteristic of a practical electrostatic fusion reactor. Mathematically such large current amplifications are possible. Whether they are experimentally accessible or dynamically stable remains to be determined.

VI. THE EXPERIMENTS

A. The Apparatus

A number of experimental devices have been constructed and operated. The model described below is characteristic of these devices and was utilized for most of the tests to be discussed. It is worth noting that many of these results have been reproduced on many occasions with a number of other tubes.

The design philosophy initially adopted[24] involved the use of symmetrically placed ion guns to provide pencil-shaped ion beams. It was felt that this arrangement would be a workable substitute for the uniform ion source assumed in the analysis. On the cathode opposite each ion gun, an open port permitted ion passage into the central cavity. Since many ions will

[24] P. T. Farnsworth, Patent No. 3,258,402 issued 28 June 1966, and patents pending.

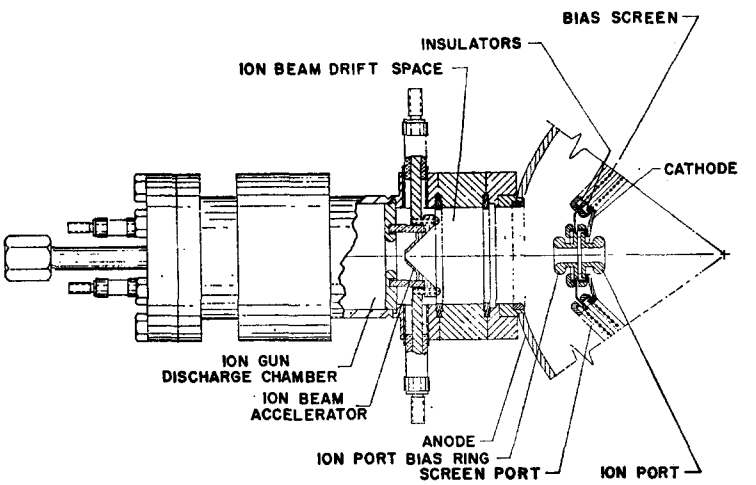

FIG. 9. The ion gun–cathode arrangement showing a typical cathode bias arrangement.

strike the real cathode structure and produce secondary electrons, initially no auxiliary electron source was provided within the cathode. This technique of electron production is simple but has two significant disadvantages. First, an expenditure of many tens of keV is required to generate a single electron. Second, the number of electrons emitted is a function of the cathode surface properties and cannot be varied during operation.

The tube assembly is shown in Fig. 8, and a typical cathode is shown in cross section in Fig. 9. The cathode, which can be operated up to 150-kV negative, is nominally 11.4 cm in diameter and has been fabricated of either 304 stainless steel or aluminum. The anode sphere was 17.8 cm in diameter and was fabricated of 304 stainless. Six symmetrically disposed ports on the anode were utilized to connect six ion guns, which have taken various forms.[25] Two viewing ports, a large cathode access port, and a vacuum-pump connection were also provided.

The cathode is rigidly mounted on a support insulator. The high-voltage connector, which coaxially houses a number of insulated leads, attaches to the top of the cathode. This connector is mounted on a plate on a 10-cm-high, fluted insulator. The insulator is immersed in an oil bath to increase its breakdown potential. The upper limit on the operating potential was not imposed by insulator breakdown but rather by field emission surging and breakdown in the small anode–cathode interelectrode space.

Since electron leakage from the cathode to the anode represents a useless and bothersome energy loss, all cathode ports are equipped with a bias assembly. As shown in Fig. 9, these biased elements are in the form of an additional ring at the ion entry ports or an additional screen at the screen ports. The energy to operate this cathode bias system was provided by a 1-kV power supply isolated and fed by an isolation transformer insulated to 150 kV. By varying the power to the primary of this transformer, the bias potential could be varied at will by the operator.

To demonstrate the effect of this arrangement and to determine the bias-potential requirements, a series of tests were performed at constant ion current, variable cathode potential, and variable bias potential. The results of these studies show that maximum current reduction occurs with biases of -500 to -1000 V. Beyond these bias potentials the tube-current reductions are negligible, indicating essentially complete electron cutoff. The bias level must increase with increasing cathode potential, since it is the field from the interelectrode space which fringes into the cathode and withdraws electrons.

The apparatus operates at steady voltage and current. Its impedance is determined and controlled by the ion current from the ion guns. Each ion gun[25] is capable of up to about 10 mA. The total current therefore has been limited to about 60 mA.

The experimental study of this inherently nonuniform ionized gas presents some unique problems. First, the discharge is confined within a high-voltage cathode situated within a grounded anode. Since the cathode must inhibit electron leakage into the interelectrode space, all viewing ports or windows must be of an appropriate structure, which is very limiting for many studies. Second, the environment of a high-voltage discharge is plagued with corona induced noise, making it difficult to shield sensitive instruments from the associated noise pickup. Third, the discharge is inherently nonuniform. Therefore, the information obtained from techniques which measure average properties is not easily interpreted. Further, the dimensions over which large density variations occur are very small (of the order of millimeters), making good spatial resolution very difficult.

[25] Initially Penning-type ion guns were utilized. Later a low-pressure arc-type gun was developed. See R. L. Hirsch and G. A. Meeks, Rev. Sci. Instr. **38**, 621 (1967).

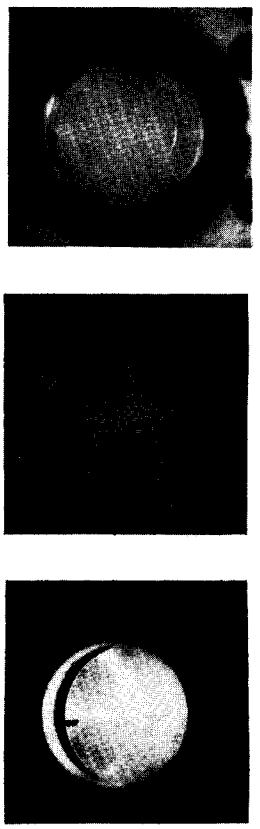

FIG. 10. Photographs of the interior of the cathode at -50 kV and various deuterium pressures.

B. Visual and Optical Observations

The device has been operated over the pressure range from 10^{-2} Torr of deuterium (the maximum operating pressure limited by interelectrode breakdown) to 10^{-5} Torr of deuterium (limited by existing pump capabilities). In Fig. 10 the appearance of the discharge at the center of the cathode is shown at three different pressure at -50 kV and 20 mA. At 8×10^{-3} Torr deuterium the ion beams are clearly evident due to excitation of the background gas by the energetic ions and the "beam-riding" electrons. Superimposed upon this pattern is a diffuse spherical cloud. As the pressure is reduced, the luminosity of the beams and center is reduced due to the decreased number of neutrals. The relative intensity of the beams with respect to the spherical cloud is also seen to decrease.

It is difficult to correlate these observations with the characteristics of the poissor described above. This is due to the following complications:

1. Maximum neutral gas excitation is produced by either high kinetic-energy deuterons or low kinetic-energy electrons.[26] Where a charge separation occurs, it is difficult to establish which species is causing the observed excitation.

2. Ionizations will occur in those regions of the ion beams where the ions have appreciable kinetic energies. The electrons resulting from these events will tend to remain in the beam.[27] If the beam ions actually come to rest at a virtual anode, these electrons would continue through the virtual anode with high kinetic energies, thereby producing additional excitations along the path of the original ion beam. Whereas a decrease in ion-induced excitation will occur near a virtual anode, this decrease will be masked by the excitation caused by the beam-riding electrons.

3. Being a region of high, positive space charge, a virtual anode is an excellent trap for low-energy electrons. Electrons so confined will cause a significant number of excitations, thereby masking an otherwise dim region.

Photographs of the discharge with and without spectral filters show no discernible variations. Discharges with neon have been observed but did not yield any significant pattern variations.

C. Neutron-Output Characteristics

If appreciable currents of deuterium or deuterium and tritium ions are utilized in these experiments, a significant fusion rate results. This rate is conveniently monitored by measuring the associated fast neutrons. A number of detectors have been utilized for this purpose, including foils, scintillators, ^{3}He proportional counters, and ionization chambers. These have been calibrated with a Ra–Be fast neutron source (1.35×10^5 neutrons/sec).

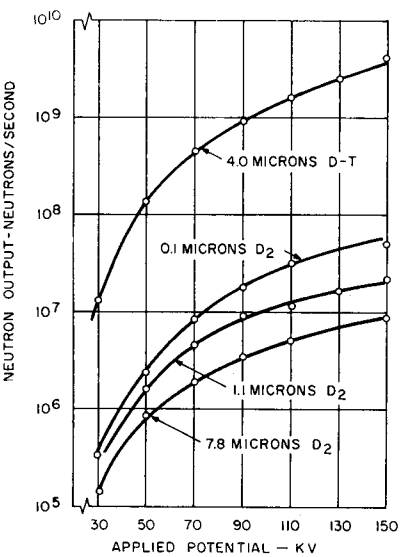

Fig.11. Neutron outputs vs applied potential at various pressures (ion current = 10 mA).

[26] See for instance C. F. Barnett, J. A. Ray, and J. C. Thompson, "Atomic and Molecular Collision Cross Sections of Interest in Controlled Thermonuclear Research," ORNL-3113, revised August 1964.

[27] See for instance A. S. Halsted and D. A. Dunn, J. Appl. Phys. **37**, 1810 (1966).

The neutron output from the apparatus is steady and reproducible. Operating times are limited only by overheating of the cathode, which is not equipped with auxiliary cooling. The output represents a combination of center and wall count, and has been found to vary with the ion current, the cathode potential, and the background gas pressure. At a given potential and gas pressure, the neutron output increases linearly with ion current. If the efficiency of ion trapping were independent of the magnitude of the ion current, the neutron output would vary as the square of the ion current. Since the dependence is linear, a square-root dependence is indicated experimentally. This is probably due to the fact that space-charge spreading in the beams scatters a portion of the ions out of an acceptable trapping cone. Improved beam optics should alleviate this problem and result in improved ion utilization.

At a given ion current and background gas pressure the neutron output increases with increased cathode potential. The dependence on potential at various gas pressures and 10-mA current is shown in Fig. 11. At pressures of the order of microns, the charge exchange and ion-neutral scattering losses are high. Reduction of the tube pressure reduces these losses and results in higher neutron yields as shown in the figure. Although the charge exchange rate was thereby decreased, neutralization of the ion beams by background gas ionization also was reduced.[27] The subsequent space-charge spreading in the ion beams results in a poorer utilization of the input, i.e., a reduction in ion-trapping efficiency.

Neutron-collimation studies have been performed to confirm the neutron origin.[28] The results of the neutron collimation studies are shown in Fig. 12 for an operating point of 90 kV, 20 mA, and 8 μ of deuterium. The diameter of the circular acceptance area of the collimator was very nearly 1.2 cm. The scanning plane intersected two opposing cathode ion-gun apertures, each located at about 3.8 cm from the tube center. Since minor peaks occur at these positions, the highest wall bombardment, should occur near there. The peak of emission on the center line is pronounced and cannot represent wall count, as there were circular screened ports in the cathode at that scanning position. This experiment therefore establishes the existence of a peak in the neutron emission in a region where a minimum in wall count would be expected.

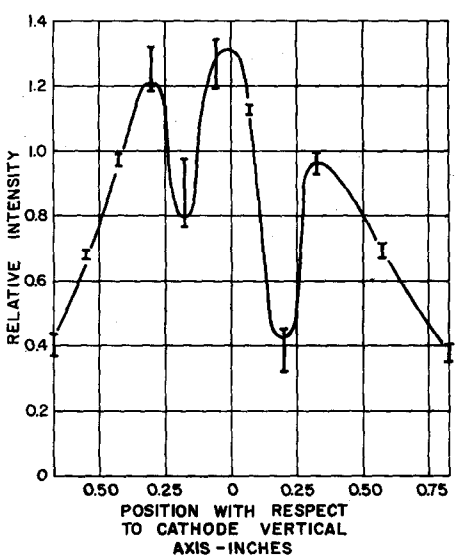

FIG. 12. The results of a neutron collimation study at −90 kV, 20 mA, and 8 μ of deuterium.

[28] Experiment performed on a bell-jar model of similar construction to the apparatus shown in Fig.8.

TABLE I. Ion densities for a D–T center fusion rate of 2×10^{10} neutrons/sec and a monoenergetic ion distribution.

Volume of fusing gas	Relative ion energies	
	10 keV	100 keV
0.1 cm³	3.2×10^{14}	1.1×10^{13}
1.0 cm³	1.0×10^{14}	3.6×10^{12}
10 cm³	3.2×10^{13}	1.1×10^{12}

From the measured neutron outputs an estimate can be made of the average ion density in the region of the fusions. This has been done for a monoenergetic ion distribution at both 10 keV and 100 keV and for several volumes of practical interest. The resultant ion densities are between 10^{12} and 10^{14} cm^{-3} as shown in Table I. Although admittedly crude estimates, they are believed to bracket the probable mean density.

D. Gamma Collimation Study

If the experimental device is operating in the manner suggested by the analysis, a maximum of bremsstrahlung emission must exist near the virtual anodes, since it is in these regions that the electrons have their maximum kinetic energies and the ion densities are the greatest. To study the spatial variations of the bremsstrahlung emission, a gamma collimator was constructed of three parallel 0.43-cm-thick lead sheets spaced 7.6 cm and 10 cm apart. Three 0.132-cm-diam holes were drilled on line in the plates. A NaI scintillation crystal coupled to an RCA 6292 phototube was placed behind the last hole. The entire detector assembly was housed in a lead cylinder to shield against reflected x rays. The schematic of the assembly and its position with respect to the cathode[28] is shown in Fig. 13. The axis of view traversed the center of the nearest cathode-screen port, and the collimator was rotated in the vertical plane so that the viewing cone terminated on solid cathode wall on the far side. The resulting plane of view unfortunately did not pass through the center of the cathode but did avoid any x rays which might have been produced on the anode adjacent to the screened port on the far side of the cathode.

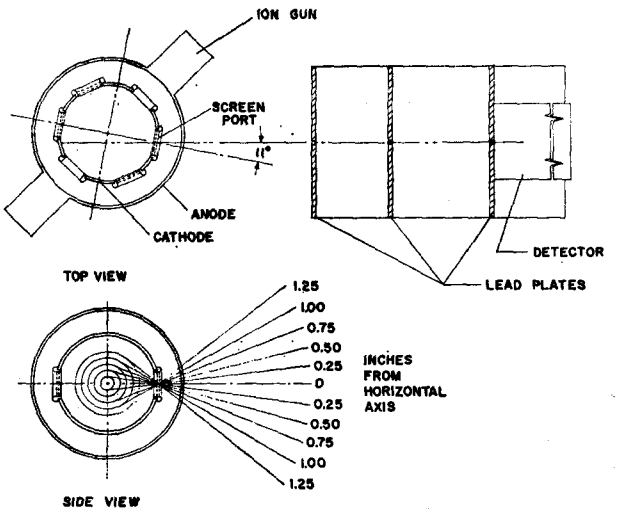

FIG. 13. The geometry and arrangement of the gamma collimation experiment.

The output from the scintillator was accumulated on a scalar, after processing through a single channel analyzer, which rejected all counts near the system noise level. Since repositioning of the collimator was done manually, frequent tube shutdown and restart were required. Although the behavior of the device was found to be extremely reproducible, small changes in power-supply settings could have affected the results. Therefore, a reference counter was used for normalization. The results of one such scan for operation at 90 kV and 20 mA are shown in Fig. 14. Peaks in intensity are found at 0.76 cm on either side and near the center. These peaks are interpreted to represent the emission maximum which would be evident when viewing tangent to a virtual anode shell. (It has been assumed that the nonisotropic nature of the bremsstrahlung emission will have a negligible effect on these results.) Since the scanning plan does not intersect the tube center, the outer peaks actually occur at about 1.26 cm. Although the results apparently indicate a virtual anode at the tube center, an inner virtual cathode could exist near these and not be observed in the scanning plane. Scans through other planes have also exhibited peaks at 1.26 cm from the center, indicating a reasonably symmetric pattern.

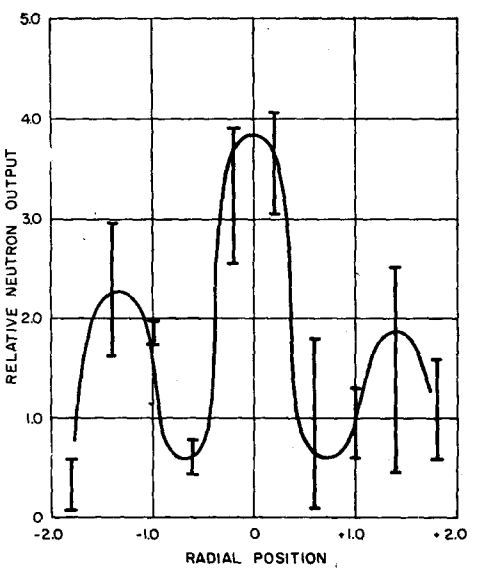

FIG. 14. The results of the gamma collimation experiment.

If indeed the peaks represent bremsstrahlung emission from virtual anodes, a question arises regarding the large size indicated by the outer peaks. The current input was 20 mA. From theoretical considerations such a low current should result in virtual anode sizes orders of magnitude smaller than observed. However, if significant ion trapping occurs a high, interior ion circulatory current could exist and thereby produce the large observed diameter. If such a situation does occur, then the role of ion input during steady operation is simply one of replenishing ion-leakage losses. Such an explanation is subject to further study.

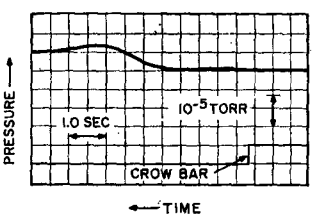

FIG. 15. The pressure variation after sudden shutdown of the properly operating tube from −50 kV and 20 mA.

E. The Quantity of Confined Gas

When the main power supply is crowbarred during normal operation in the 10^{-5}-Torr region, a modulation of the tube pressure is indicated on the Varian milli-Torr pressure gauge. The first pressure increase is small and appears immediately. A second increase appears about 2 sec later. An example of these variations is shown in Fig. 15. The amplitude of the second change varies roughly as the square root of the cathode current, as shown in Fig. 16. The second pulse is believed to represent the release of gas confined within the cathode. The observed delay is curiously long and cannot be explained in terms of instrument delay or of the gas diffusion times.

In order to verify that the second release was associated with confinement, the cathode was purposely misaligned so that the ion beams entered the cathodic volume but did not result in a center formation. The apparatus was then operated in exactly the same manner as before. A representative pressure variation after crowbar in this mode is shown in Fig. 17. A slight increase in pressure is noted immediately after shutdown, but no secondary release is observed.

The probable explanation for the large time delay is as follows. When the apparatus is crowbarred, a dropping bar short circuits the cathode to the anode in a time of the order of milliseconds. The confined gas senses this change in two ways. First, the ion current into the cathode is cut off, since the field in the interelectrode space accelerates ions from the guns. Second, electrons returning to the cathode from the center will find the cathode at a more positive potential. Therefore, the electron currents which were previously balanced become unbalanced. This combination of events results in the sudden conversion of the potential energy of ions in the virtual anode(s) to kinetic energy. This being the case, the ions in the virtual anode(s) strike the cathode with significant kinetic energies. In so doing these ions penetrate into the cathode, rediffuse to the surface, and leave as neutrals. Thus, a pulse of gas should occur after crowbar in a time determined by the diffusion properties of the cathode wall.

The penetration of 50-keV D^+ ions in aluminum is about 5000 Å. According to Dushman,[29] the time constant for gases in metals is roughly

$$T \simeq (4/\pi^2)(a^2/D), \qquad (26)$$

where a is the characteristic length (cm) and D is the diffusion coefficient (cm²/sec). Unfortunately no data on the diffusion of deuterium in aluminum was found. However, Smithells[30] gives experimental data which indicates that diffusion coefficient of hydrogen in aluminum is roughly 600 times smaller than the diffusion of hydrogen in nickel. At 165°C the diffusion coefficient for hydrogen through nickel is about 10^{-7} cm²/sec. Accordingly, the approximate deuterium diffusion coefficient in aluminum is 1.67×10^{-10} cm²/sec at 165°C, and the diffusion time for 5000 Å is $T_{165°} \simeq 6$ sec.

The observed delay and the calculated time constant are of the same magnitude, tending to support the original hypothesis. The magnitude of the observed pressure rises are of the order of 1.0×10^{-5} Torr. Since the volume of the vacuum system is of the order of 40 liters, this increase represents the release of about 10^{16} molecules. If one or more virtual anodes have been created, this large gas release could be reconciled with the lower densities indicated for the fusion regions by the neutron outputs. The square root of current dependence indicated in Fig. 16 strengthens the arguments with regard to the ion-trapping efficiency.

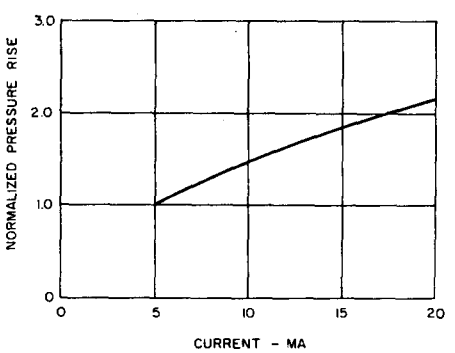

FIG. 16. The indicated gas release vs ion current.

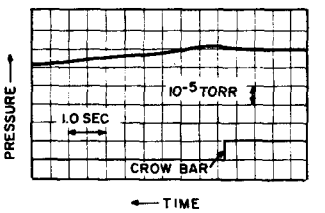

FIG. 17. The pressure variation after sudden shutdown of the tube when a center has not formed.

F. rf Behavior

The absence of a magnetic field eliminates a large class of possible instabilities. Those which remain are of an electrostatic nature. In an effort to locate and identify any such disturbances, a Lavoie Laboratories type 19 spectrum analyzer was coupled to the discharge within the cathode. This coupling was accomplished by allowing electrons from within the cathode to leak into the interelectrode space and bombard an insulated probe positioned on the anode vessel. This probe was coupled to the analyzer directly through single- and multiple-loop antennas and through resistive loads. A 25-Mc/sec bandwidth was utilized and the range from 10 Mc/sec to 44 Gc/sec was covered with each coupling technique. The only signals observed were in the form of random noise pattern over the entire spectrum. No coherent or large amplitude signals were evident.

A Tektronix 531 oscilloscope was utilized to cover the region below 10 Mc/sec. The only modulations indicated were associated with power-supply ripple.

If any gross oscillations or instabilities were present within the cathode, their presence should have been manifested by a modulation of the leaking electron beam. Since no gross modulation was apparent, it was concluded that the discharge in its present form is stable.

G. A Probe Study

If either a nude or an insulated probe is placed near the center of the cathode sphere, the spherical glow will not form. If the discharge is initially not collision dominated this phenomenon is not surprising, since the presence of a macroscopic object will obviously shorten the free paths and alter the nature of the formation.

[29] S. Dushman, *Scientific Foundations of Vacuum Technique* (John Wiley & Sons, Inc., New York, 1962).

[30] C. J. Smithells, *Gases and Metals* (Chapman and Hall, Ltd., Aberdeen, Scotland, 1938).

A distinctly different discharge can be produced within the apparatus at higher pressures, i.e., $1–2\times 10^{-2}$ Torr. This mode is the well-known collision-dominated, hollow-cathode discharge.[31] Insertion of a probe into this discharge results in an almost negligible change in its appearance. Although the probe could not provide quantitative information, its destructive effect implies that the original discharge is not collision dominated.

VII. SUMMARY AND CONCLUSIONS

The Poisson equation was solved numerically assuming monoenergetic ion and electron distributions and radial flow in spherical geometry. Time dependence was excluded. All ions were assumed emitted from an outer anode, and all electrons were assumed emitted from an ion permeable inner cathode. A large number of the resultant potential distributions were found to be spatially periodic and to exhibit extremely high electric fields near the center of the sphere. These interesting potential structures were characterized by the alternate formation of virtual anodes and virtual cathodes and were called poissors. The associated radial focusing resulted in an approximately $1/R^2$ particle pressure dependence. Therefore, near the center of the sphere a high-density, high-pressure region exists which may be of thermonuclear interest.

A series of experiments were performed in order to test the theoretical predictions. Copious neutron emissions were observed, a part of which was determined to originate from the luminous, spherical central region. Estimates of the central ion density corresponding to the observed fusion rates range from 10^{12} to 10^{14} cm^{-3}. The gas released upon high-voltage crowbar represented of the order of 10^{16} molecules. The differences in these two ion densities may be attributable to the formation of two or more virtual anodes.

A bremsstrahlung collimation study indicated a spatially periodic symmetric emission pattern which was interpreted as representing the formation of at least two virtual anodes. A probe placed in the active discharge was found to destroy it, indicating that the discharge was originally not collision dominated. An electron leak from the cathode was utilized to search for instabilities. In the range up to 44 Gc/sec, no pronounced signals above noise were detected, suggesting that the discharge is stable.

The experimental observations suggest that a poissor-like structure has been formed and is the source of a significant fraction of the observed neutron output. Whether this concept is capable of being scaled to a useful fusion reactor remains to be established. The fact that the confinement region appears stable is encouraging. Under any conditions much interesting physics is represented by these concepts and merits a great deal of further study.

(*Note Added in Proof*: Recent preliminary one- and two-dimensional computer experiments performed by D. Dunn, C. Barnes, and R. Hockney (Stanford University) show that a number of apparently stable configurations exist wherein virtual anodes and cathodes are formed in cylindrical and spherical geometries).

ACKNOWLEDGMENTS

The author is deeply indebted to Dr. P. T. Farnsworth, Rear Admiral F. R. Furth, and International Telephone and Telegraph Corporation for their encouragement and support of this work.

The author appreciates useful discussions with George W. Bain, G. A. Meeks, and many of the scientific personnel of the ITT Industrial Laboratories. The technical assistance of G. A. Meeks and D. Barr was invaluable in the performance of the experiments.

[31] J. Litton and H. L. L. van Paassen, Ann. Conf. Phys. Electron., 23rd, March 1963; E. C. Muly, Ann. Conf. Phys. Electron, 34 March 1964; C. Popovici, M. Somesan, and V. Nistor, Phys. Letters **22**, 587 (1966).